BBA - Biomembranes 1869 (2027) 184584

Contents lists available at ScienceDirect

BBA - Biomembranes

journal homepage: www.elsevier.com/locate/bbamem

Mechanisms of lipid recognition in methyl-α-cyclodextrin-mediated lipid exchange for the design of plant plasma membrane models☆

Christine Cézard [a], Magali Deleu [b], Benjamin Bouvier [c,*]

[a] Laboratoire de Glycochimie et des Agroressources d'Amiens, UR 7378, Université de Picardie Jules Verne, UFR des Sciences, 33 rue Saint Leu, Amiens Cedex 80039, France
[b] Laboratory of Molecular Biophysics at Interfaces, TERRA Teaching and Research Centre, Gembloux Agro-Bio Tech, University of Liege, 2, Passage des Déportés, 5030 Gembloux, Belgium
[c] Enzyme and Cell Engineering, CNRS UMR7025/Universié de Picardie Jules Verne, 33 rue Saint Leu, Amiens Cedex 80039, France

ARTICLE INFO

Dataset link: https://sdrive.cnrs.fr/s/3LdoZ8Bqp9mMLDT

Keywords:
Cyclodextrin
Lipid exchange
Plant plasma membrane
Free energy
Molecular dynamics

ABSTRACT

Asymmetric liposomes that mimic plant plasma membranes (PPM) have not been developed so far, despite the impact of the PPM's transverse lipid distribution on its biophysical properties and its involvement in many biological processes. The cyclodextrin-mediated exchange of PLPC (16:0-18:2 PC) and POPC (16:0-18:1 PC), two lipids that are strongly represented in the PPM, can potentially be used to achieve an asymmetry in leaflet composition mimicking that of the PPM. In this work, we use molecular free energy simulations to study the interaction of methyl-α-cyclodextrins with these two lipids. We show that kinetic barriers to the sliding of the CD along the linoleoyl chain of PLPC, due to the locking effect of curved linoleoyl chain conformations, can extend the lifetime of PLPC/CD complexes compared to POPC. While sufficient to discriminate PLPC from POPC, the associated free energy barriers show that CD uptake and release is feasible for both lipids within the typical timescales of *in vitro* experiments. The preferred positions of the CD on the lipid chains also condition the ability to recruit additional CDs for better shielding of the lipid tails from water. We discuss how this subtle kinetic balance relates to previous experimental results and its implication for the design of PPM models via lipid exchange.

Contents

1. Introduction 2
2. Methods 2
 2.1. Conformational coordinate 2
 2.2. Simulation parameters 3
 2.3. Simulating the sliding of a CD along the lipid chains 3
 2.4. Simulating the lipid/CD_4 complexes 4
 2.5. Analyses 4
3. Results and discussion 4
 3.1. Differences in CD affinities for linoleoyl and oleoyl chains 4
 3.2. Uptake of multiple CDs on PLPC and POPC 6
4. Concluding remarks 7
CRediT authorship contribution statement 7
Declaration of competing interest 7
Acknowledgments 7
Appendix A. Supplementary data 7
Data availability 8
References 8

☆ This article is part of a Special issue entitled: 'Cellular Membranes' published in BBA - Biomembranes.

* Corresponding author.
E-mail address: benjamin.bouvier@u-picardie.fr (B. Bouvier).
URL: http://www.benjamin-bouvier.fr (B. Bouvier).

https://doi.org/10.1016/j.bbamem.2026.184584
Received 17 March 2026; Received in revised form 27 October 2026; Accepted 4 November 2026
Available online 12 November 2026
0005-2736/© 2026 The Author(s). Published by Elsevier B.V. This is an open access article under the CC BY license (http://creativecommons.org/licenses/by/4.0/).

1. Introduction

Cyclodextrins (CD) are macrocycles composed of α-D-glucopyranose units linked by α-(1,4) glycosidic bonds. They form circular frusta with a hydrophilic exterior and relatively nonpolar interior, whose character can be further modulated by functionalization [1]. CDs have emerged as a powerful tool for the selective extraction and delivery of lipids: indeed, their hydrophilic outer surface allows them to navigate the aqueous phase between lipid membranes, while their hydrophobic inner cavity provides a shielded environment for the inclusion of lipophilic guest molecules [2]. Consequently, CDs have been used to manipulate the composition of lipid bilayers: by exchanging specific lipids between initially symmetric donor and acceptor vesicles, they can produce model bilayer systems with defined lipid asymmetry mimicking the non-uniform distribution of lipids in mammalian and bacterial plasma membranes [3–7].

The process of CD-mediated lipid exchange can be decomposed into a succession of events [8,9]. The first step strongly depends on the lipid headgroup. Some (such as phosphatidylinositol) form specific complexes with certain CD types [10,11], assisting the extraction of individual lipids which transiently project out of the membrane due to thermal fluctuations. Conversely, other lipid types (such as phosphatidylcholines) rely on the overall destabilization of the membrane by nonspecific electrostatic interactions with CDs, especially at higher concentrations [12,13]. In the second step, the focus of lipid-CD interactions shifts to the acyl chains, which need to be shielded from the solvent [14]; the CD:lipid stoichiometry also comes into play at this point, since long acyl chains require multiple CDs to be completely covered [15–17]. The resulting complex becomes a soluble entity capable of reaching the acceptor vesicle via spontaneous diffusion, where the lipid is released after reconstructing native interactions with the target bilayer. Other types of lipids can be transported in the opposite direction by CDs, achieving the required compositional anisotropies in both vesicles after multiple rounds of bidirectional exchanges.

The CD-mediated lipid exchange in bilayers and liposomes is powered by differences in the specificity of the CDs for different lipid types. However, the relationship between the lipid binding affinities of CDs and their efficiency for lipid exchange is complex. Intuitively, a reversible binding is required to allow the release of lipids into their target vesicle, implying that the underlying CD-lipid interactions cannot be too strong. This ensures that, provided a sufficient CD concentration is available and equilibrium can be reached, the lipid exchange will eventually equilibrate the lipid compositions of donor and acceptor vesicles. In addition, the differences in relative affinities of CDs for specific lipid types are most likely constrained: the uptake and release of a lipid with a much higher CD affinity would be prioritized over that of other lipid species, slowing down the net rate of exchange [18]. Most experimental studies on CD-mediated lipid exchange only document the macroscopic outcome of these subtle competitive processes. Their molecular characterization, essential to guide design choices in lipid exchange experiments, is still incomplete, despite valuable additions from the small number of studies on specific systems cited in the previous paragraphs [8,11,13,16,17].

The primary determinant of cargo specificity in CDs is the size of the cavity. Naturally occurring α, β and γ-CDs consist of an increasing number of sugar moieties (respectively six, seven and eight), resulting in progressively larger cavity diameters. γ-CDs specialize in the encapsulation of larger macrocycles or multiple smaller guests [19]. β-CDs have been successfully used for lipid exchange but have an undesirable side-effect: their high affinity for cholesterol [20], which they tend to remove from the target membranes, requires the latter to be subsequently reintroduced [7]. Conversely, the small cavity of α-CDs is only large enough to accommodate a single lipid acyl chain [21], making it an ideal candidate for lipid recognition and exchange. Furthermore, alkyl or hydroxyalkyl substituent groups can lengthen the CD torus, enhancing the binding with larger lipophilic compounds such as acyl chains (a process termed hydrophobic extension) [16,22]. Indeed, methyl-α-CDs (M-α-CD) have been successfully used to replace endogenous phospholipids in mammalian cell plasma membranes [23]. Generally, for α as for β-CDs, the rates of exchange of long and unsaturated acyl chains have been observed to be lower than that of shorter, saturated chains [4–6,23–26]. Incidentally however, studies on β-CDs have shown the lipid affinity of these CDs to increase with the number of unsaturations [21,27].

In this work, we focus on the exchange of two lipid types: 1-palmitoyl-2-oleoyl-sn-glycero-3-phosphocholine (16:0-18:1 PC, POPC), and 1-palmitoyl-2-linoleoyl-sn-glycero-3-phosphocholine (16:0-18:2 PC, PLPC) using permethylated α-CD. Along with glycosylinositol phosphorylceramides (GIPC), these lipids have been used to create promising models of the plant plasma membrane (PPM) [28]. The PPM has not received as much attention as its mammalian counterpart despite its crucial role for the regulation of nutrients and the response to cellular environment via signal transduction. It predominantly features 16:0-18:2 lipids: linoleic acid represents up to 60 % of fatty acid content, compared to less than 15 % in the mammal plasma membrane [29]. Like the latter, however, the PPM features an asymmetric distribution of lipids between its inner and outer leaflets which remains understudied, despite its implications for biological processes [30,31]. In the mammalian plasma membrane, POPC tends to favor the more tightly packed environment of the apoplastic (outer) leaflet, while PLPC congregates with other polyunsaturated lipids in the more fluid cytosolic (inner) leaflet [32,33]. The PPM is expected to feature a similar distribution, favored by the preferential interactions of the outer leaflet GIPC with saturated and monounsaturated components such as POPC [34,35]. Thus, asymmetric PPM model vesicles could potentially be obtained by using M-α-CDs to exchange POPC and PLPC between symmetrical vesicles mimicking the composition of either leaflet of the PPM. However, unlike for β-CD, not much is known about the interaction of lipids with M-α-CDs at the molecular level. Consequently, this paper uses atom-level molecular simulations to quantitatively explore the free energy landscape of the PLPC/POPC/M-α-CD interactions, by characterizing the sliding of one or several permethylated CDs along the chains of isolated lipid molecules solvated in water, taking into account the entropic effects associated with the relative flexibility of the lipid chains. It assesses the feasability of one of the crucial steps of the PLPC-POPC exchange process and suggests atom-level justifications for previously reported experimental results, such as the slower exchange rate of unsaturated lipids by α-CDs, the influence of alkyl chain flexibility thereupon, or the accomodation of multiple CDs per lipid chain experimentally suspected to occur at higher CD concentrations.

2. Methods

2.1. Conformational coordinate

In this work, we defined a conformational coordinate termed λ to represent the position of a CD molecule on a lipid chain in a way that is easy to understand, robust to conformational changes, computationaly differentiable, and implementable within the PLUMED software package [36]. It was then used to study the sliding of one or more CD molecules along the acyl chains of PLPC and POPC in enhanced sampling molecular dynamics (MD) simulations. The coordinate λ was defined as follows (Fig. 1):

1. The “top” and “bottom” of the lipid chain were respectively defined as the α carbon of the ester group connecting the chain to the headgroup (often termed C_2 in lipid nomenclature), and the final carbon atom of the chain (atoms C_{18} for linoleoyl/oleoyl and C_{16} for palmitoyl chains).

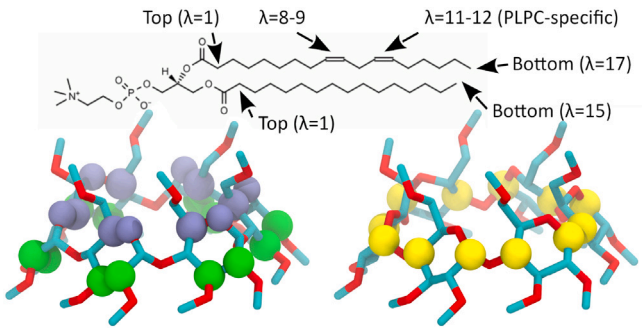


Fig. 1. Definition of the conformational coordinate λ. Top: values of λ over the linoleoyl and palmitoyl chains of PLPC (the oleoyl and palmitoyl chains of POPC have the same number of carbon atoms and are numbered similarly). Bottom left: small-rim (blue spheres) and large-rim (green spheres) atoms used to define the CD axis. Bottom right: atoms used to define the CD center (yellow spheres). Carbon and oxygen atoms are represented as cyan and red sticks, respectively, and hydrogen atoms are omitted.

2. The unit vector of the CD axis was defined as passing through the geometrical centers of the small and large rim atoms of the CD (Fig. 1, bottom right): The direction of the vector was chosen so that it pointed toward the top of the lipid chain; depending on the sense of insertion of the CD on the chain (small or large rim first), this could require the vector to be multiplied by -1.
3. Each carbon atom of the lipid chain was projected onto the CD axis. Atoms "above" the CD have a positive projection, those "below" a negative projection. Since the lipid chain is flexible and can potentially loop back around the CD, this information was propagated along consecutive carbon atoms starting from the bottom, making sure that only one transition from "below" to "above" can exist.
4. The center of the CD was defined as the geometrical center of the atoms shown on the bottom right panel of Fig. 1.
5. The CD center was projected onto each of the bonds linking consecutive lipid chain carbon atoms. Bonds for which both carbons were determined in point 3 to be above the CD contribute 1 to the conformational coordinate λ; those for which both carbons are below the CD do not contribute. The bond on which the CD currently sits has one carbon above, the another one below; it contributes the ratio between the value of the projection and the length of the bond.

Defined in this way, the conformational coordinate λ varies continuously from 1 to 17 from the top to the bottom of linoleoyl and oleoyl chains, and from 1 to 15 for palmitoyl chains. It is equal to i when the projection of the CD center on the chain is located on carbon atom i; when the center falls between two carbon atoms i and $i+1$, it equals i plus the ratio between the distance of the projected center to atom i and the length of the C_i-C_{i+1} bond. λ is differentiable with respect to the position of the CD atoms and can thus be used as biasing coordinate in enhanced sampling MD simulations (see below). As mentioned in point 3 above, this definition of λ is robust to any conformational changes of the lipid chain, including cases in which it loops back around the CD. It was implemented inside PLUMED version 2.9.4.

2.2. Simulation parameters

The structures and force field parameters for permethylated α-CD, POPC and PLPC were taken from the Q4MD-CD [37] and LIPID11 [38] forcefields. All simulations were performed at a constant temperature of 300 K, imposed using a velocity rescaling thermostat coupled separately to the solute and solvent ($\tau = 0.1$ ps). Constant-pressure simulations used an isotropic Parrinello-Rahman barostat (reference pressure 1 bar, compressibility 4.5×10^{-5} bar^{-1}, $\tau = 5$ ps). All lipid/CD complexes were solvated in TIP3P water, inside truncated octahedral unit cells with a buffer distance of 10 ∀ from the solute to the edge of the cell. Periodic boundary conditions were used in all 3 dimensions of space. Short-range Coulomb and van der Waals forces were cut off at 10 ∀, while long-range electrostatics were computed with the particle-mesh Ewald scheme. In all simulations, the length of bonds between hydrogen and non-hydrogen atoms were constrained and the integration timestep was chosen as 2 fs. All simulations were performed using GROMACS [39] version 2024.3, combined with PLUMED for umbrella sampling simulations and the post-processing of trajectories with respect to λ.

2.3. Simulating the sliding of a CD along the lipid chains

The free energy landscape for the sliding of a permethylated α-CD, inserted from its small-rim or large-rim side (see Fig. 1), along the acyl chains of a single POPC or PLPC lipid solvated in water was simulated using umbrella sampling simulations [40]. They consist in independent simulations (called "windows"), in each of which the CD is restrained around a given position on the lipid chain using a harmonic restraint acting on the conformational coordinate λ. The complete FEP can be reconstructed from the distributions of λ values in all windows, provided the distributions in consecutive windows overlap, using the weighted histogram analysis method [41]. The statistical uncertainties associated with the FEP were calculated from Monte Carlo bootstrap analyses.

For the PLPC linoleoyl and POPC oleoyl chains and for each of the two possible insertion sides of the CD, 33 windows with λ values ranging from 1 to 17 with a stride of 0.5 were used. For the palmitoyl chains of both lipids, only small-rim CD insertion was considered; 29 windows with λ values ranging from 1 to 15 with a stride of 0.5 were used. Each window consisted in a 50 ns simulation at constant temperature and pressure, during which a harmonic restraining potential of 50 kJ mol^{-1} acting on λ and centered on the window's reference λ value was applied and the instantaneous value of λ was recorded every picosecond. A total of 190 windows were thus simulated, representing a total simulation time of 9.5 μs.

The starting conformations for the umbrella sampling windows were obtained as follows. For each of the lipid chains and CD insertion senses considered, a series of 20 reasonable conformations of the lipid/CD complex spanning all positions of the CD over the chain were manually constructed using LeaP [42] and solvated in water. The solvated systems were minimized and simulated with position restraints on the solute heavy atoms for 1 ns at constant volume and 1 ns at constant pressure; the position restraints were progressively removed over 5 ns and the systems were simulated for 50 ns each. The value of λ over the conformations of these 20 trajectories was recorded every picosecond. From the set of conformations thus obtained, conformations with λ values matching those of the umbrella sampling windows were extracted and used as starting conformations for these windows. Although no rigorous proof of the complete sampling of the conformational subspace orthogonal to λ can be provided (an issue common to all similar free energy studies), the span and convergence of the interchain angle distributions (see below) indicate that this selection of starting conformations is adequate considering the total simulation time of more than 1.5 μs per lipid chain. For the simulation of the isolated lipids, the sets of conformations from the umbrella sampling simulations of PLPC and POPC were classified into 20 clusters based on the conformation of the lipid; the lipid structure representative of each cluster was solvated, equilibrated and simulated for 100 ns using the previously mentioned protocol (a total production simulation time of 2 μs per lipid).

2.4. Simulating the lipid/CD_4 complexes

Two CD molecules were manually inserted on each of the acyl chains of PLPC and POPC using LeaP. The small rim of the topmost CD on each chain was oriented toward the lipid headgroup, whereas both insertion directions were tested for the lower CDs. The resulting lipid/CD_4 complexes were energy-minimized, solvated in TIP3P water, simulated with position restraints on the solute heavy atoms for 1 ns at constant volume then 1 ns at constant pressure; the position restraints were progressively removed over 5 ns and the two systems were simulated for 1 μs. The positions of each of the four CDs on their respective chains, as defined by the four associated coordinates λ, were recorded every picosecond. To prevent the CDs from being released from the acyl chains and diffusing away, an upper wall on λ was imposed for values strictly greater than 17 (resp. 15) for the linoleoyl/oleoyl (resp. palmitoyl) chains, using a harmonic potential (stiffness 1000 kJ mol^{-1}); this is necessary to achieve an exhaustive sampling of all possible CD positions and the convergence of the underlying FEPs. The FEPs were calculated from Gaussian kernel density estimations of the distribution $\rho(\lambda)$ of the combined values of the four λ series, associated with the four CD molecules, over the simulations (the overlap between the distributions of λ values for the two CDs on a chain was checked). The FEPs were obtained as $\Delta G = -RT \ln \rho(\lambda)$, where R is the ideal gas constant and T the temperature (RT = 0.5962 kcal mol^{-1} at T = 300 K). The statistical uncertainties associated with the FEPs were calculated from Monte Carlo bootstrap analyses. Twenty simulations of 50 ns (ten for each lipid type) starting from slightly different atomic coordinates and velocities were also performed without the upper wall constraint on λ, to observe the lability of the lower CD units on each chain.

2.5. Analyses

Mass-weighted radii of gyration (R_g) and root-mean-square fluctuations (RMSF) were computed over the entire length of the umbrella sampling windows using the GROMACS analysis toolset. The reference state for RMSF was the average structure of the acyl chain over each window. The angle between the two chains of a lipid molecule was calculated from the arc cosine of the inner product of the average of the normalized vectors connecting consecutive carbon atoms on each chain. Monte Carlo bootstrap analyses [43] were performed using the WHAM implementation by Grossfield [44]. 100 Monte Carlo trials per simulation window were performed and a decorrelation time of 10 ps was used (estimated from the average autocorrelation time of λ series). Molecular graphics were generated using VMD version 1.9.3 [45]. All plots were performed using Matplotlib version 3.10.8 [46].

3. Results and discussion

3.1. Differences in CD affinities for linoleoyl and oleoyl chains

In this work, we study the interaction free energy between M-α-CD and the POPC and PLPC acyl chains, which conditions the ability of the CD to shield these chains from the solvent, in turn affecting the transport and exchange of the lipids between PPM model vesicles. We assume the first phase of the process, which consists of the extraction of a lipid from the donor membrane and the initial binding of the CD, to be complete. As previously mentioned, depending on the nature of the lipid headgroup this process can be directly assisted by the CD or originate from a more global, CD-facilitated destabilization of the membrane. Nevertheless, while PLPC and POPC share the same headgroup, their respective packing properties within the donor membrane might affect their relative ease of extraction. We also do not consider the possible recapture of CDs after their release from the chains, which could play an important role but would be extremely difficult to adequately sample.

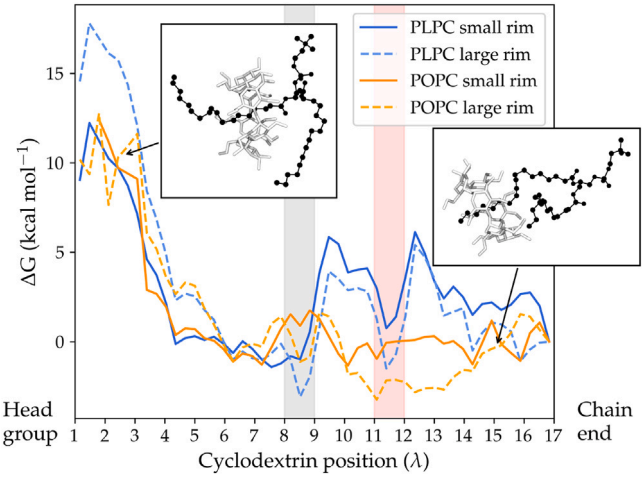


Fig. 2. Free energy (ΔG) profiles for the sliding of a CD (inserted through its small or large rim) along the unsaturated acyl chains of POPC and PLPC, showing the barriers caused by the combination of two unsaturations in PLPC compared to POPC. The CD position is given in terms of the acyl chain carbon atom indices, using the conformational coordinate λ (see Section 2 and Fig. 1). Representative conformations of CD/POPC complexes are shown as insets (black spheres: lipid; white rods: CD). Each FEP is determined up to an additive constant; these were chosen to equalize all four FEPs at position 17. The positions of the unsaturations are highlighted (gray: common to PLPC and POPC; red: specific to PLPC).

In inclusion complexes of M-α-CD on the acyl chains of PLPC and POPC, the CD can potentially slide along the lipid chain, locally reducing its conformational plasticity. Studying this mechanism can reveal potential preferred interaction positions of the CD on the chains and quantify the free energy barriers between these positions and the chain extremity, which can affect the kinetics of CD recruitment or release. To study this mechanism, we simulated the sliding of the M-α-CD, inserted through either its small-rim or large-rim side, along the linoleoyl and oleoyl chains of PLPC and POPC (which distinguish these lipids from one another) using a technique called umbrella sampling MD (see Section 2 for details). Umbrella sampling explores the sliding motion of the CD along the chain in a piecewise manner, by combining multiple simulation "windows" in each of which the CD is restrained around a specific position on the chain. It yields the associated FEP, which includes the contribution of variations in conformational entropy, a driving force behind many important mechanisms in large flexible molecules [47]. As a reference, the sliding motion of a CD along the saturated palmitoyl chain common to both lipids was studied with the same technique. The combined simulation time was 9.5 μs, which allows to extensively sample the relevant conformational space along the chosen coordinate. The resulting sliding FEPs for both lipids and both CD insertion directions are presented on Fig. 2. The convergence of the FEPs was verified on subsets of the total window simulation lengths (Supporting Information figure S1) and the statistical uncertainties evaluated using Monte Carlo bootstrap analyses (figure S2). The sliding FEP along the palmitoyl chains are presented on figure S3 and their convergence and statistical uncertainties on figure S4.

The FEPs reveal that the sliding of the CD along PLPC is hampered by free energy barriers located beneath each of the unsaturated positions. When the CD is bound at the top of the PLPC chain ($\lambda \leq 7$), it must overcome a significant initial barrier of up to 7 kcal mol^{-1} to move beyond the first unsaturation, and a second, lower barrier to continue past the second unsaturation, before it can be released. Conversely, when the CD moves upwards from the bottom end of the chain upon initial contact, the barriers are lower (3 to 4 kcal mol^{-1}) but still relevant. Strikingly, while POPC shares the first unsaturation

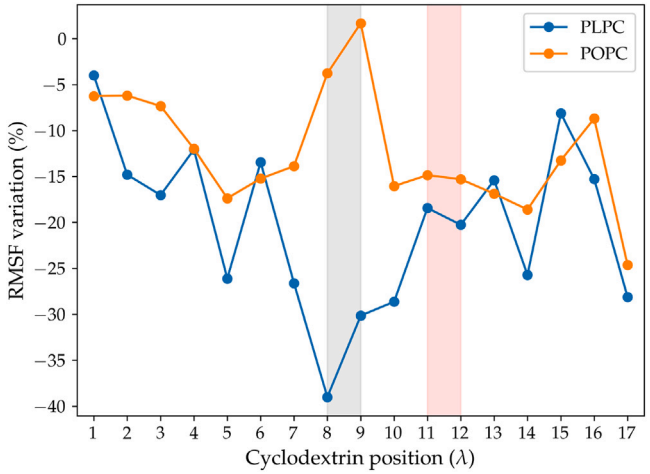


Fig. 3. Variation in the flexibility of the unsaturated lipid chain of PLPC or POPC upon the passage of the CD, measured as the percentage of variation of the RMSF of the carbon atom at the CD position from its value in the isolated lipid. The positions of the unsaturations are highlighted (gray: common to PLPC and POPC; red: specific to PLPC).

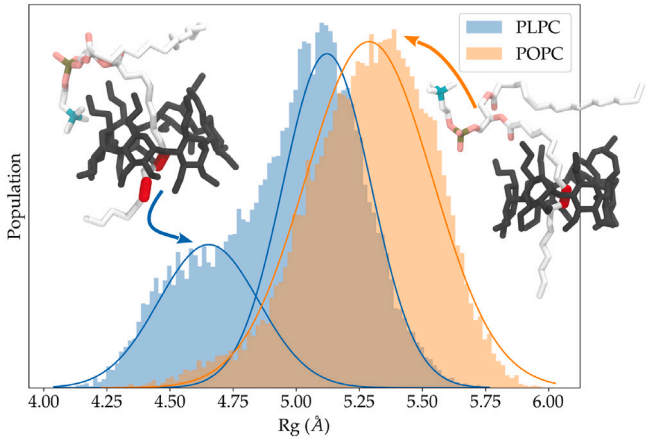


Fig. 4. Conformational statistics for the unsaturated lipid chain of PLPC or POPC, as histograms of R_g values in conformations for which the CD is located over the topmost unsaturation (common to both lipids). The Gaussian mixture deconvolutions of the histograms, showing bimodal (resp. monomodal) behaviors for PLPC (resp. POPC) are plotted as solid lines. Representative conformations of PLPC/CD (left) and POPC/CD (right) complexes at two frequently encountered R_g values are shown as insets (CD: black sticks; lipid: remaining sticks, color-coded by atom type; the unsaturations on the lipid tail are highlighted in red).

with PLPC, no barrier to sliding can be observed at the corresponding position for the former. The FEP for POPC is relatively flat, indicating that the CD can freely move back and forth along the oleoyl chain. This behavior is identical to the one observed for the fully saturated palmitoyl chains of both POPC and PLPC.

However, according to transition state theory (which is frequently used to provide orders of magnitude of conformational transition kinetics in biological systems [48]), free energy barriers of 4 kcal mol^{-1} and 7 kcal mol^{-1} respectively take less than a nanosecond and a few milliseconds to be overcome at 300 K [49] (assuming a transmission coefficient of 0.1 to 0.01 typically associated with friction in liquids). Considering the diffusive nature of CD sliding, these timescales should be considered as orders of magnitude rather than actual rates; however, they suggest with reasonable confidence that the PLPC linoleoyl chain can readily bind and release CDs within the timescales of typical *in vitro* exchange experiments despite slower binding kinetics than the oleoyl or palmitoyl chains. In fact, the slight asymmetry of the PLPC FEP, with a barrier to release that is 3 kcal mol^{-1} higher than to uptake, could help mitigate PLPC's slower binding kinetics: in a competitive environment featuring PLPC, POPC, and a default concentration of CDs, the CDs will remain more durably complexed to PLPC and thus not be completely monopolized by POPC. This could be interpreted as a higher affinity of M-α-CD for polyunsaturated chains, similar to findings on β-CDs [21], that similar simulations of chains with three or more insaturations would be required to confirm. To summarize, the energetics of M-α-CD binding kinetically discriminate the linoleoyl chain of PLPC from the oleoyl chain of POPC but allow both to be transported (an essential specification for lipid exchange, as mentioned in the introduction). It should also be noted that the sense of insertion of the CD on the linoleoyl and oleoyl chains has little impact on the underlying free energy landscape — the relative affinity for both acyl chain types is preserved in both insertion modes (which justifies why only one insertion direction was investigated for the palmitoyl chains). This lack of preference entropically favors the recruitment of CDs and explains their efficiency for the exchange of lipids.

To investigate the origins of the differences between the sliding FEPs on the unsaturated chains of PLPC and POPC, we examined how the CD locally affects the flexibility of each lipid chain around its current position. We compared the root mean square fluctuations (RMSF) of each carbon atom in the presence and absence of the CD (Fig. 3). We found that, on average, the CD causes the carbon chain to locally become 15 to 25 % more rigid in order to avoid steric clashes within the CD cavity. However, the region of the first unsaturation behaves very differently in both lipids: no rigidification is required for the CD to pass through this region on POPC, while for PLPC the local flexibility must be reduced by 40 %. This is required because polyunsaturated acyl chains like PLPC have been shown to possess greater flexibility than more saturated ones, due to the extended conformational space available to saturated carbons sandwiched between two double bonds [50,51]. Reducing the conformational space available to a system is entropically unfavorable, which points to a strong entropic contribution to the sliding free energy barriers observed for PLPC. Finally, the similarity of the sliding FEPs for the oleoyl and palmitoyl chains show that a single unsaturation does not expand the conformational space of an alkyl chain sufficiently to hamper the sliding of a CD, even as tight-fitting as M-α-CD, and the similar FEPs for the palmitoyl chains in both lipids reveal no underlying collective conformational effects between the two chains of these lipids.

To further characterize the origins of the rigidification of both acyl chains, we examined the folding of the unsaturated lipid chains observed during our simulations when the CD was positioned over the topmost unsaturation, common to PLPC and POPC. Fig. 4 illustrates the distributions of the lipid chain radii of gyration (R_g) over the relevant conformations. R_g is a measurement of the distribution of atoms in the lipid with respect to its center of mass, and reflects the general shape (globular or elongated) of the molecule. For POPC, the R_g distribution shows a single peak at high values, indicating the prevalence of extended linear chain conformations that facilitate CD sliding. Conversely, the R_g distribution for PLPC is shifted toward smaller values and has a significant (based on the fit quality of Gaussian mixture deconvolution analyses) secondary peak around 4.6 ∀, corresponding to conformations where the chain bends away from the CD axis, locking the CD on the chain by preventing its sliding. Because the carbons at the two unsaturations are close to each other, their conformations are strongly correlated, which propagates the rigidification induced by the CD's passage from one unsaturation to the other. This collective effect increases the statistical weight and lifespan of folded structures, explaining the previously discussed free energy barriers.

3.2. Uptake of multiple CDs on PLPC and POPC

Experimental evidence on the sequestering of lipids by CDs points toward a mechanism in which a single CD forms a 1:1 complex with a lipid following the extraction of the latter from the membrane; only then are additional CDs recruited by the lipid [24,52]. Indeed, a single CD is not large enough to shield the entirety of a lipid acyl chain from water by itself, even considering the hydrophobic extension brought about by possible alkyl substituents on the CD [16,17,22]. Depending on the CD and lipid types, typical CD:lipid stoichiometries of 4:1 to 6:1 have been postulated (2 to 3 CDs per chain, 6 to 8 carbon atoms per CD) [15,52]. Although a thorough isolation of the hydrophobic acyl chains from water will favor the diffusion of the encapsulated lipid toward the target bilayer, in the context of lipid exchange the efficient release of the lipid at destination must not be hampered by multiple bound CDs. Another question of interest is whether the additional CD units modify the relative kinetic stabilities of the complexes compared to their 1:1 counterparts studied above.

To shed light on these points, we have performed MD simulations on solvated PLPC and POPC complexed by four CD units (two CDs on each of the two acyl chains). Initial unbiased simulations revealed a great lability of the CD units at the bottom of both the saturated and the unsaturated chains of both lipids, which were found in many instances to spontaneously dissociate from the chains within time spans of a few tens of nanoseconds and either diffuse away or be recaptured by the chain. Over multiple simulations, this outcome was found to be independent on the direction of insertion of the lower CD units but particularly likely for PLPC compared to POPC. Because achieving an exhaustive sampling of the complete process would be too computationally demanding, we restricted our study to the exploration of the kinetic stability of the preformed lipid/CD_4 complex by using a biasing potential to prevent the CDs from fully dissociating from the chains. This potential consists in an "upper wall" on the conformational coordinate λ, which does not bias the system as long as the CDs remain over the chains. The FEPs associated with the positions of the CDs were then evaluated from the density of states observed during extensive 1 μs simulations (see Section 2 for details); they are presented on Fig. 5. The convergence of the FEPs with simulation times, the associated statistical uncertainties and overlap of the position densities of both CDs on a chain are shown on Supporting Information figure S5 and S6. The FEPs only convey a partial picture of the overall stability of lipid/CD_4 complexes, which does not include the influence of release and capture events and should thus be interpreted with caution; however, they provide valuable information on the respective capacities of the chains to accommodate multiple CD units at experimentally postulated stoichiometries, which do impact the propensity of the complexes to form.

The FEPs confirm the observations made on the set of unbiased lipid/CD_4 simulations. For both PLPC chains, the free energy decreases from position 12 until the end of the chain, confirming the propensity of the second CD to spontaneously leave the chain. This is not observed for POPC, in which the unsaturated oleoyl chain "traps" the lower CD around position 14. From there, the barrier to dissociation is only 2 kcal mol^{-1}; nevertheless, spontaneous release is expected to be slower than for PLPC. Comparatively, while the final part of the palmitoyl chain of POPC has a flat FEP and does not actively retain the CD, it does not facilitate its release as does the matching chain on PLPC. The reason for these differences is apparent when looking at the preferred position of the first CD (corresponding to the regions of lowest free energy on the FEPs): it tends to sit much lower on the PLPC chains (right at the first unsaturation, around position 8) compared to POPC (where it shows a marked preference for position 4). This shift in the position of the first CD toward the end of the chain in PLPC leaves less room for the second CD, sterically "pushing" it to dissociate. A similar behavior, albeit less strongly marked, is also apparent for the palmitoyl chains of both lipids. Interestingly, the FEP for the second CD on the PLPC linoleoyl chain (from positions 12 to 17) is quite comparable to the sliding FEP of a single CD on this same chain (Fig. 2): the presence of the first CD does not modify the free energy landscape, but disfavors the additional CD by occupying the only durably stable position on it. On the contrary, in POPC, the first CD occupies the top of the oleoyl chain and leaves much more room for the second unit; the latter can freely move between positions 12 and 17, which entropically stabilizes its binding. The sliding FEP of a single CD on the POPC oleoyl chain (Fig. 2) is thus significantly altered by the presence of the first CD. The opposite is true for the palmitoyl chains: while POPC retains the relatively flat profile associated with the sliding of a single CD, the FEP for the unsaturated chain of PLPC features a non-negligible free energy barrier at the same position as the one on the linoleoyl chain, hinting at the existence of interchain collective effects which can potentially alter the binding selectivity observed experimentally for CDs on isolated fatty acids. To summarize, the interchain and intrachain collective effects tend to amplify the conformational preferences observed for a single CD and result in higher labilities of the lower CDs for PLPC compared to POPC, suggesting that complexes with high CD:lipid stoichiometries may be less favorable for the former than the latter.

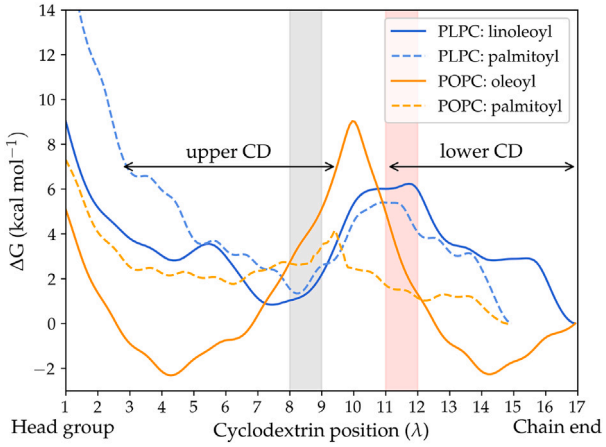


Fig. 5. Free energy (ΔG) profiles for the position of the two CDs on each of the acyl chains of PLPC and POPC. For clarity, the ranges of positions most frequently observed for each CD, corresponding to regions of lower free energies on the PMFs, are materialized with double arrows. The unsaturated positions are highlighted (gray: common to PLPC and POPC; red: specific to PLPC).

To better understand the reasons behind the preference of the CDs for distinct zones on the acyl chains in complexes with multiple CDs, the angles between the unsaturated and palmitoyl chains in PLPC and POPC were monitored in the presence of four CDs, a single CD, and in the isolated lipids (Fig. 6 — the convergence of the angle distributions with simulation time can be found on Supporting Information figure S7). The isolated lipids showed no preferential relative orientation of the acyl chains; they alternate between "closed" conformations where both chains are parallel (typically observed within a bilayer) and "open" conformations where the chains extend away from one another. A similar distribution was observed in the presence of a single CD on the unsaturated chain, although a slight shoulder becomes apparent toward closed (resp. open) conformations for PLPC (resp. POPC). Strikingly however, when both acyl chains bear two CD units each, PLPC strictly favors closed conformations while POPC is predominantly open. This explains the relative positioning of the upper CDs on the unsaturated chains: in POPC, the CD sits close to the lipid headgroup, penalizing closed conformations due to steric clashes with the upper CD on the palmitoyl chain; in PLPC, on the other hand, closed conformations are sterically possible and weakly stabilized by interactions between CDs on both chains. However, because hydrogen

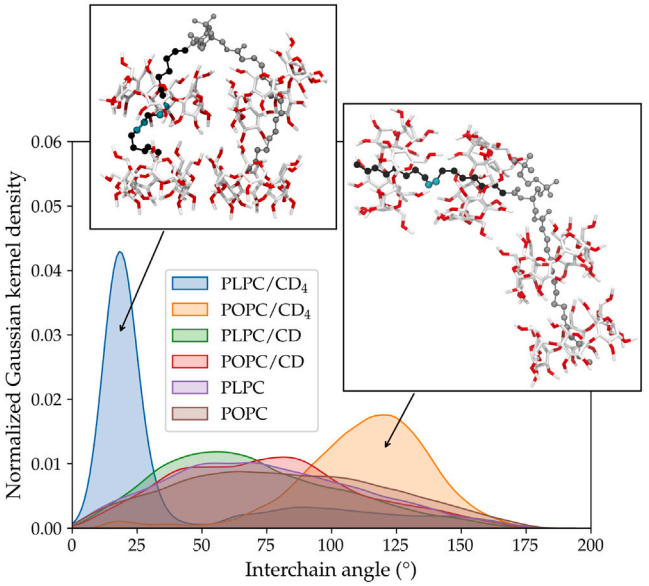


Fig. 6. Distributions of angles between acyl chains in PLPC and POPC, when complexed by 4 CDs, 1 CD, or isolated (as normalized Gaussian kernel densities). Representative conformations of lipid/CD_4 complexes are shown as insets. Lipids: black (unsaturated chain), cyan (unsaturated carbons) and gray (remainder) spheres; CDs: white (carbon) and red (oxygen) rods.

bonds are not readily available on methylated CDs, these interactions are not strong enough to prevent the dissociation of the lower CDs on both chains of PLPC. In fact, the motion of both chains causes friction between the lower CDs, which contributes to driving them off the chain. Interactions between the two close-lying PLPC alkyl chains also explain the emergence of the matching free energy barrier at λ=10-12 on the palmitoyl chain.

These findings have several implications for the M-α-CD-mediated lipid exchange mechanism. On the whole, they tend to support previous experimental results reporting higher affinities [21] and slower exchange kinetics [24] for CDs on unsaturated acyl chains, but reveal that the explanation lies in a complex interplay of kinetics and thermodynamics involving collective effects. They also highlight the role of conformational entropy, via the restriction of both intrachain and interchain conformational space induced by the CDs, in this subtle balance. However, in the context of lipid exchange, PLPC's preference for closed conformations, once complexed with several CDs, could hypothetically facilitate its extraction from the donor membrane and its reinsertion into the acceptor membrane. The lability of the lower CDs results in an accrued exposure of parts of the acyl chains to the solvent, limiting diffusion speed. On the other hand, the extended, rod-like POPC/CD_4 complexes, although more stable due to the limited lability of the lower CDs, are also much less compact and prone to transverse drag, which also limits diffusion. In addition, PLPC is also favored by the slower dissociation kinetics of the first CD, which is much less labile than its counterpart on POPC; PLPC can thus more durably recruit part of the CD population for its transport. Under the competitive conditions brought about by low CD concentrations, this might give the edge to PLPC and favor its transport over that of POPC. Acting on M-α-CD concentration could thus be a way of adjusting the composition of the target bilayers, as was recently observed for M-β-CDs: high CD concentrations cause "empty" CDs to actively extract lipids from the outer leaflet, while low concentrations result in oversaturated CDs inserting their cargos into this leaflet [53]. In our case, low M-α-CD concentrations would thus favor the extraction of PLPC from the outer leaflet; switching to higher concentrations would then favor the insertion of POPC, achieving the desired asymmetry. However, we remind that our study focuses on part of the exchange process only and comparison with experiments thus remains indicative; in particular, a complete account of concentration-dependent effects should incorporate the release and recapture of CDs rather than limit itself to preformed complexes as we do here.

4. Concluding remarks

Although CD-mediated lipid exchange has been used for a few decades and the relative affinities of lipids for different CD are mostly known, a lot of this knowledge remains empirical and few molecular interaction studies provide a justification thereof. In particular, accurate free energy differences quantifying the thermodynamic and kinetic preferences of CDs for lipid types are severely lacking. In this work, we show that M-α-CD discriminates between saturated, mono and diunsaturated chains via a complex combination of kinetics and thermodynamics which involves collective effects between multiple CDs. Nevertheless, the kinetic preference for POPC is not sufficiently strong to completely inhibit the exchange of PLPC. M-α-CDs seem well suited for the generation of asymmetric models matching the transverse distribution of 16–18 lipids in the PPM. However, obtaining a complete picture of the process would require the simulation of CD/membrane interactions, crucial during the initial steps of lipid extraction from the donor membrane and which could mitigate the CD/lipid affinities reported herein. Lipid-dependent packing properties, for instance, can limit the lipid exchange kinetics by favoring or hindering lipid extraction [21]; however, higher CD concentrations can modulate this effect by locally destabilizing local packing properties [8]. We are currently combining experiments and coarse-grained MD to achieve this goal. Meanwhile, our current model remains one of the most detailed to date and provides valuable insights into the driving force behind CD-mediated lipid exchange, that reach beyond our work by justifying previous experimental observations.

CRediT authorship contribution statement

Christine Cézard: Writing – original draft, Methodology, Investigation. **Magali Deleu:** Conceptualization. **Benjamin Bouvier:** Writing – original draft, Supervision, Software, Methodology, Investigation, Conceptualization.

Declaration of competing interest

The authors declare that they have no known competing financial interests or personal relationships that could have appeared to influence the work reported in this paper.

Acknowledgments

The calculations presented herein were performed using HPC resources from the *Université de Picardie Jules Verne* MatriCS computing platform. M. Deleu thanks the F.R.S.-FNRS (Belgian Fund for Scientific Research) for her position as research director and their support via the PDR project Surfasymm (grant T.0063.19).

Appendix A. Supplementary data

Supplementary material related to this article can be found online at https://doi.org/10.1016/j.bbamem.2026.184584.

Convergence checks and statistical uncertainties of FEPs on Figs. 2 and 5. Sliding FEPs along the palmitoyl chains of PLPC and POPC. Convergence of the angular distributions on Fig. 6.

Data availability

A sample PLUMED configuration file, defining the con- formational coordinate λ for the sliding of M-α-CD (inserted through its large rim) along the linoleoyl chain of PLPC can be downloaded at https://sdrive.cnrs.fr/s/3LdoZ8Bqp9mMLDT. Additional simulation data can be provided upon request.

References

[1] T. Loftsson, D. Duchene, Cyclodextrins and their pharmaceutical applications, Int. J. Pharm. 329 (1–2) (2007) 1–11.
[2] M.A. Esteso, C.M. Romero, Cyclodextrins: properties and applications, Int. J. Mol. Sci. 25 (8) (2024) 4547.
[3] M. Markones, A. Fippel, M. Kaiser, C. Drechsler, C. Hunte, H. Heerklotz, Stairway to asymmetry: five steps to lipid-asymmetric proteoliposomes, Biophys. J. 118 (2) (2020) 294–302.
[4] M. Doktorova, F.A. Heberle, B. Eicher, R.F. Standaert, J. Katsaras, E. London, G. Pabst, D. Marquardt, Preparation of asymmetric phospholipid vesicles for use as cell membrane models, Nat. Protoc. 13 (9) (2018) 2086–2101.
[5] M. Markones, C. Drechsler, M. Kaiser, L. Kalie, H. Heerklotz, S. Fiedler, Engineering asymmetric lipid vesicles: accurate and convenient control of the outer leaflet lipid composition, Langmuir 34 (5) (2018) 1999–2005.
[6] Q. Lin, E. London, Preparation of artificial plasma membrane mimicking vesicles with lipid asymmetry, in: D. Holowka (Ed.), PLoS One 9 (1) (2014) e87903.
[7] P. Suresh, E. London, Using cyclodextrin-induced lipid substitution to study membrane lipid and ordered membrane domain (raft) function in cells, Biochim. Biophys. Acta, Biomembr. 1864 (1) (2022) 183774.
[8] C.A. López, A.H. de Vries, S.J. Marrink, Molecular mechanism of cyclodextrin mediated cholesterol extraction, in: M. Berkowitz (Ed.), PLoS Comput. Biol. 7 (3) (2011) e1002020.
[9] W. Khuntawee, P. Wolschann, T. Rungrotmongkol, J. Wong-ekkabut, S. Hannongbua, Molecular dynamics simulations of the interaction of beta cyclodextrin with a lipid bilayer, J. Chem. Inf. Model. 55 (9) (2015) 1894–1902.
[10] F. Fauvelle, J. Debouzy, S. Crouzy, M. Göschl, Y. Chapron, Mechanism of α-cyclodextrin-lnduced hemolysis. 1. The two-step extraction of phosphatidylinositol from the membrane, J. Pharm. Sci. 86 (8) (1997) 935–943.
[11] S. Crouzy, F. Fauvelle, J.-C. Debouzy, M. Göschl, Y. Chapron, Investigation of the α-cyclodextrin-myo-inositol phosphate inclusion complex by NMR spectroscopy and molecular modeling, Carbohydr. Res. 287 (1) (1996) 21–35.
[12] V. Bernat, C. Ringard-Lefebvre, G. Le Bas, S. Lesieur, Action of α-cyclodextrin on phospholipid assemblies, J. Incl. Phenom. Macrocycl. Chem. 57 (1–4) (2007) 113–119.
[13] R. Zappacosta, B. Cornelio, S. Pilato, G. Siani, F. Estour, M. Aschi, A. Fontana, Effect of the incorporation of functionalized cyclodextrins in the liposomal bilayer, Molecules 24 (7) (2019) 1387.
[14] F. Fauvelle, J. Debouzy, R. Nardin, A. Gadelle, Nuclear magnetic resonance study of a polar headgroup determined α-cyclodextrin-phospholipid association, Bioelectrochem. Bioenerg. 33 (1) (1994) 95–99.
[15] L. Szente, J. Szejtli, J. Szeman, L. Kato, Fatty acid-cyclodextrin complexes: Properties and applications, J. Incl. Phenom. Mol. Recognit. Chem. 16 (4) (1993) 339–354.
[16] C. Vargas, C. Schönbeck, I. Heimann, S. Keller, Extracavity effect in cyclodextrin/surfactant complexation, Langmuir 34 (20) (2018) 5781–5787.
[17] P. F. Garrido, M. Calvelo, R. Garcia-Fandiño, Á. Piñeiro, Rings, hexagons, petals, and dipolar moment sink-sources: The fanciful behavior of water around cyclodextrin complexes, Biomolecules 10 (3) (2020) 431.
[18] Z. Huang, E. London, Effect of cyclodextrin and membrane lipid structure upon cyclodextrin–lipid interaction, Langmuir 29 (47) (2013) 14631–14638.
[19] G. Kali, S. Haddadzadegan, A. Bernkop-Schnürch, Cyclodextrins and derivatives in drug delivery: new developments, relevant clinical trials, and advanced products, Carbohydr. Polym. 324 (2024) 121500.
[20] R. Zidovetzki, I. Levitan, Use of cyclodextrins to manipulate plasma membrane cholesterol content: Evidence, misconceptions and control strategies, Biochim. Biophys. Acta, Biomembr. 1768 (6) (2007) 1311–1324.
[21] L. Szente, É. Fenyvesi, Cyclodextrin-lipid complexes: cavity size matters, Struct. Chem. 28 (2) (2016) 479–492.
[22] R. De Lisi, G. Lazzara, S. Milioto, N. Muratore, Characterization of the cyclodextrin−surfactant interactions by volume and enthalpy, J. Phys. Chem. B 107 (47) (2003) 13150–13157.
[23] G. Li, J. Kim, Z. Huang, J.R. St. Clair, D.A. Brown, E. London, Efficient replacement of plasma membrane outer leaflet phospholipids and sphingolipids in cells with exogenous lipids, Proc. Natl. Acad. Sci. USA 113 (49) (2016) 14025–14030.
[24] J. Debouzy, F. Fauvelle, S. Crouzy, L. Girault, Y. Chapron, M. Göschl, A. Gadelle, Mechanism of α-cyclodextrin induced hemolysis. 2. A study of the factors controlling the association with serine-, ethanolamine-, and choline-phospholipids, J. Pharm. Sci. 87 (1) (1998) 59–66.
[25] E.K. Fridriksson, P.A. Shipkova, E.D. Sheets, D. Holowka, B. Baird, F.W. McLafferty, Quantitative analysis of phospholipids in functionally important membrane domains from RBL-2H3 mast cells using tandem high-resolution mass spectrometry, Biochemistry 38 (25) (1999) 8056–8063.
[26] V. Kainu, M. Hermansson, P. Somerharju, Introduction of phospholipids to cultured cells with cyclodextrin, J. Lipid Res. 51 (12) (2010) 3533–3541.
[27] J. Wang, J.-L. Zhang, F.-A. Wu, Enrichment process for α-linolenic acid from silkworm pupae oil, Eur. J. Lipid Sci. Technol. 115 (7) (2013) 791–799.
[28] N. Monnier, A. Furlan, S. Buchoux, M. Deleu, M. Dauchez, S. Rippa, C. Sarazin, Exploring the dual interaction of natural rhamnolipids with plant and fungal biomimetic plasma membranes through biophysical studies, Int. J. Mol. Sci. 20 (5) (2019) 1009.
[29] F. Furt, F. Simon-Plas, S. Mongrand, Lipids of the plant plasma membrane, in: The Plant Plasma Membrane, Springer Berlin Heidelberg, 2010, pp. 3–30.
[30] R. Clarke, K. Hossain, K. Cao, Physiological roles of transverse lipid asymmetry of animal membranes, Biochim. Biophys. Acta, Biomembr. 1862 (10) (2020) 183382.
[31] J. Rossy, Y. Ma, K. Gaus, The organisation of the cell membrane: do proteins rule lipids? Curr. Opin. Chem. Biol. 20 (2014) 54–59.
[32] T. Fujimoto, I. Parmryd, Interleaflet coupling, pinning, and leaflet asymmetry—Major players in plasma membrane nanodomain formation, Front. Cell Dev. Biol. 4 (2017).
[33] D. Marquardt, B. Geier, G. Pabst, Asymmetric lipid membranes: Towards more realistic model systems, Membranes 5 (2) (2015) 180–196.
[34] A. Mamode Cassim, P. Gouguet, J. Gronnier, N. Laurent, V. Germain, M. Grison, Y. Boutté, P. Gerbeau-Pissot, F. Simon-Plas, S. Mongrand, Plant lipids: Key players of plasma membrane organization and function, Prog. Lipid Res. 73 (2019) 1–27.
[35] J. Gronnier, P. Gerbeau-Pissot, V. Germain, S. Mongrand, F. Simon-Plas, Divide and rule: Plant plasma membrane organization, Trends Plant Sci. 23 (10) (2018) 899–917.
[36] G.A. Tribello, M. Bonomi, D. Branduardi, C. Camilloni, G. Bussi, PLUMED 2: new feathers for an old bird, Comput. Phys. Comm. 185 (2) (2014) 604–613.
[37] C. Cézard, X. Trivelli, F. Aubry, F. Djedaïni-Pilard, F.-Y. Dupradeau, Molecular dynamics studies of native and substituted cyclodextrins in different media: 1. Charge derivation and force field performances, Phys. Chem. Chem. Phys. 13 (33) (2011) 15103.
[38] A.A. Skjevik, B.D. Madej, R.C. Walker, K. Teigen, LIPID11: a modular framework for lipid simulations using amber, J. Phys. Chem. B 116 (36) (2012) 11124–11136.
[39] M.J. Abraham, T. Murtola, R. Schulz, S. Páll, J.C. Smith, B. Hess, E. Lindahl, GROMACS: High performance molecular simulations through multi-level parallelism from laptops to supercomputers, SoftwareX 1 (2015) 19–25.
[40] J. Kästner, Umbrella sampling, Wiley Interdiscip. Rev.: Comput. Mol. Sci. 1 (6) (2011) 932–942.
[41] S. Kumar, J.M. Rosenberg, D. Bouzida, R.H. Swendsen, P.A. Kollman, The weighted histogram analysis method for free-energy calculations on biomolecules. I. The method, J. Comput. Chem. 13 (8) (1992) 1011–1021.
[42] D.A. Case, H.M. Aktulga, K. Belfon, I.Y. Ben-Shalom, J.T. Berryman, S.R. Brozell, D.S. Cerutti, T.E. Cheatham III, G.A. Cisneros, V.W.D. Cruzeiro, T.A. Darden, R.E. Duke, G. Giambasu, M.K. Gilson, H. Gohlke, A.W. Goetz, R. Harris, S. Izadi, S.A. Izmailov, K. Kasavajhala, M.C. Kaymak, E. King, A. Kovalenko, T. Kurtzman, T.S. Lee, S. LeGrand, P. Li, C. Lin, J. Liu, T. Luchko, R. Luo, M. Machado, V. Man, M. Manathunga, K.M. Merz, Y. Miao, O. Mikhailovskii, G. Monard, H. Nguyen, K.A. O'Hearn, A. Onufriev, F. Pan, S. Pantano, R. Qi, A. Rahnamoun, D.R. Roe, A. Roitberg, C. Sagui, S. Schott-Verdugo, A. Shajan, J. Shen, C.L. Simmerling, N.R. Skrynnikov, J. Smith, J. Swails, R.C. Walker, J. Wang, H. Wei, R.M. Wolf, X. Wu, Y. Xiong, Y. Xue, D.M. York, S. Zhao, P.A. Kollman, Amber 2022, University of California, San Francisco, 2022.
[43] B. Efron, R.J. Tibshirani, An Introduction to the Bootstrap, Chapman and Hall, Boca Raton, FL, 1993.
[44] A. Grossfield, WHAM: an implementation of the weighted histogram analysis method, 2026, version 2.1.1, https://github.com/agrossfield/wham.
[45] W. Humphrey, A. Dalke, K. Schulten, VMD: visual molecular dynamics, J. Mol. Graph. Model. 14 (1) (1996) 33–38.
[46] J.D. Hunter, Matplotlib: a 2D graphics environment, Comp. Sci. Eng. 9 (3) (2007) 90–95.
[47] G. Wei, W. Xi, R. Nussinov, B. Ma, Protein ensembles: how does nature harness thermodynamic fluctuations for life? The diverse functional roles of conformational ensembles in the cell, Chem. Rev. 116 (11) (2016) 6516–6551.
[48] A.R. Fersht, From covalent transition states in chemistry to noncovalent in biology: from β- to Φ-value analysis of protein folding, Q. Rev. Biophys. 57 (2024) e4.
[49] K.J. Laidler, M.C. King, Development of transition-state theory, J. Phys. Chem. 87 (15) (1983) 2657–2664.
[50] S.E. Feller, K. Gawrisch, A.D. MacKerell, Polyunsaturated fatty acids in lipid bilayers: intrinsic and environmental contributions to their unique physical properties, J. Am. Chem. Soc. 124 (2) (2001) 318–326.
[51] B. Antonny, S. Vanni, H. Shindou, T. Ferreira, From zero to six double bonds: phospholipid unsaturation and organelle function, Trends Cell Biol. 25 (7) (2015) 427–436.

[52] T.G. Anderson, A. Tan, P. Ganz, J. Seelig, Calorimetric measurement of phospholipid interaction with methyl-β-cyclodextrin, Biochemistry 43 (8) (2004) 2251–2261.

[53] M. Krompers, M. Jaki, S. Götz, J. Lembeck, L. Kaul, M. Holzer, H. Heerklotz, Asymmetric phase transitions in lipid bilayers: coupling or bending? Faraday Discuss. 259 (2025) 107–128.